AJNR

Assessment of whole-brain vasodilatory capacity with acetazolamide challenge at 1.5 T using dynamic contrast imaging with frequency-shifted burst.

J R Petrella, C DeCarli, M Dagli, J H Duyn, C B Grandin, J A Frank, E A Hoffman and W H Theodore

AJNR Am J Neuroradiol 1997, 18 (6) 1153-1161
http://www.ajnr.org/content/18/6/1153

Assessment of Whole-Brain Vasodilatory Capacity with Acetazolamide Challenge at 1.5 T Using Dynamic Contrast Imaging with Frequency-Shifted Burst

Jeffrey R. Petrella, Charles DeCarli, Mandeep Dagli, Josef H. Duyn, Cécile B. Grandin, Joseph A. Frank, Elizabeth A. Hoffman, and William H. Theodore

PURPOSE: To determine whether whole-brain acetazolamide-induced changes in regional cerebral blood volume (rCBV) can be assessed on a conventional gradient 1.5-T MR system using 3-D dynamic susceptibility contrast-enhanced MR imaging. **METHODS:** A 3-D frequency-shifted (FS) burst technique was used to assess the intravascular first pass of contrast agent. Changes in rCBV were calculated in 40 volunteers before and after acetazolamide (n = 30) or saline (n = 10) injection using customized analysis software on an independent workstation. A single-section gradient-echo technique with better spatial resolution was used in one additional volunteer to examine the effect of partial volume averaging on calculation of absolute rCBV. **RESULTS:** A statistically significant increase in rCBV (gray matter = 23%, white matter = 32.5%) was noted after acetazolamide compared with saline. Baseline fractional CBVs were 22% ± 3% for gray matter and 12% ± 2% for white matter. Partial volume averaging was probably responsible for a systematic but linear overestimation of absolute rCBV. **CONCLUSION:** Acetazolamide-induced changes in rCBV can be assessed using 3-D dynamic susceptibility contrast-enhanced MR imaging with FS-burst on a conventional gradient 1.5-T MR system. Values obtained with this technique overestimate absolute rCBV but are systematically biased and can be used for intersubject and intrasubject ratio comparisons.

Index terms: Blood, volume; Brain, magnetic resonance; Magnetic resonance, technique

AJNR Am J Neuroradiol 18:1153–1161, June 1997

Burst refers to a class of ultrafast magnetic resonance (MR) imaging techniques that are characterized by "bursts" of radio frequency excitation pulses. The modification frequency-shifted (FS) burst, a fast three-dimensional susceptibility-weighted MR imaging sequence, can be used for whole-brain dynamic contrast perfusion imaging on standard 1.5-T systems without specialized gradient hardware (1). Although there is a moderate sacrifice of spatial resolution compared with single-section gradient-echo (2–4) and multisection echo-planar imaging (5), FS-burst is useful for whole-brain bolus tracking, since it enables the entire brain to be scanned in approximately 2 seconds with equal T2* weighting over k-space (6). Because of its whole-brain coverage, it is possible to sample a wide range of voxels for estimating an arterial input function directly from the images; thus, absolute rather than relative regional cerebral blood volume (rCBV) measures can be obtained (7). Unlike relative rCBV values, absolute values can be compared among different examinations and subjects.

A widely available, whole-brain imaging

Received September 6, 1996; accepted after revision December 12.

Presented at the annual meeting of the Radiological Society of North America, Chicago, Ill, November 1996.

Dr Grandin was supported by a grant from the Fondation St Luc, Catholic University of Louvain, Belgium.

From the Laboratory of Diagnostic Radiology Research (J.R.P., M.D., J.H.D., J.A.F.), the National Institute of Neurological Disorders and Stroke (C.D., E.A.H., W.H.T), and the In Vivo NMR Research Center (C.B.G.), National Institutes of Health, Bethesda, Md; and the Department of Radiology (J.R.P), Hospital of the University of Pennsylvania, Philadelphia.

Address reprint requests to Jeffrey R. Petrella, MD, OD/OIR/LDRR, Building 10, Room B1N256, 10 Center Dr, MSC 1074, Bethesda, MD 20892.

AJNR 18:1153–1161, Jun 1997 0195-6108/97/1806–1153

technique yielding absolute rCBV values would be extremely useful in clinical trials comparing hemodynamic parameters in different groups of patients, as well as in evaluating pharmacologic interventions on individual patients. One useful pharmacologic intervention is a vasodilatory challenge with acetazolamide, which is important in assessing cerebrovascular reserve capacity (8–10). We evaluated the feasibility of dynamic susceptibility contrast-enhanced MR imaging with FS-burst to estimate absolute rCBV and assess whole-brain regional vasodilatory capacity with acetazolamide challenge.

Materials and Methods

Theory

I. Measurement of rCBV.—A noninvasive determination of rCBV based on indicator dilution theory has been well described (11) and depends on accurate measurement of indicator concentration as a function of time. According to this theory, relative rCBV can be determined by integrating the area beneath the time concentration curve for a given voxel or region. To obtain absolute rCBV, it is necessary to divide this area by the area under an arterial input function, as described in the equation,

$$1) \qquad V_f = \frac{\int_0^\infty c_t(t)\,dt}{\int_0^\infty c_a(t)\,dt},$$

where V_f is the fractional rCBV, $\int_0^\infty c_t(t)\,dt$ is the area under the tissue concentration time curve, and $\int_0^\infty c_a(t)\,dt$ is the area under the arterial input concentration time curve (11). Any artery on the scan that can completely encompass a single voxel may be used, in principle (11), to obtain an arterial input function. Dividing the area under the tissue time concentration curve by the area under the arterial input function curve accounts for differences in the shape of the tissue curve caused by between-patient or between-examination factors, such as different cardiac output or different injection rate, as these factors are reflected in the arterial input function.

II. Relationship between MR Signal and Contrast Agent Concentration.—For susceptibility-weighted MR imaging, regional loss in signal intensity induced by the introduction of a paramagnetic contrast agent can be converted to a measure of concentration of the contrast agent (7). Because the mechanisms governing signal loss in the presence of a paramagnetic contrast agent may be different inside tissue regions (12, 13), from which we obtain tissue time concentration curves, as opposed to large vessels, from which we obtain the arterial input function, the relationship between signal intensity and concentration of contrast agent must be examined separately in each case.

A. Within tissue. It has been empirically determined from tissue models of the capillary bed and in vivo experiments in animals that the relationship between change in signal intensity and tissue concentration of paramagnetic contrast agent canbe characterized by the following relationship for susceptibility-weighted imaging (7, 12, 14):

$$2) \qquad c(t) = -k \cdot \ln \frac{S(t)}{S(0)},$$

where $c(t)$ is the local tissue concentration of the contrast material at time t, $S(t)/S(0)$ is the fractional signal intensity change at time t from the baseline signal intensity, and k is a calibration constant related to the tissue and echo time of the pulse sequence. This relationship holds true for blood concentrations up to 1.5 mmol/L of gadopentetate dimeglumine (M. Hedehus, E. Rostrup, H. B. W. Larsson, "The Relationship between R2* and Gadolinium Concentration in Vivo," presented at the annual meeting of the International Society of Magnetic Resonance Imaging, New York, NY, April 1996).

B. Within large vessels. Such a predictable relationship between T2*-weighted signal change and contrast agent concentration given by Equation 2 should be true for the voxels within or around large vessels as well, if one is to obtain the arterial input function directly from the images. Empirical evidence from previous brain imaging work using a dual-section higher resolution T2*-weighted technique has supported the validity of extending Equation 2 to arterial voxels (15). There is also experimental evidence in dogs that justifies the validity of this relationship (L. Porkka, M. Neuder, G. Hunter, R. Weisskoff, J. Belliveau, B. Rosen, "Arterial-input function measurement with MRI," In: *Book of Abstracts 1:120, Society of Magnetic Resonance in Medicine, San Francisco, Calif, August 10–16, 1991*).

To show that the relationship between signal intensity change, as measured by our technique, and contrast concentration could also be approximated by this linear relationship for both tissue and arteries, we examined three healthy volunteers with the 3-D FS-burst imaging protocol. Each volunteer had three consecutive examinations with a fixed volume bolus injection of gadopentetate dimeglumine in three different dilutions with normal saline. The dilutions of contrast agent were 60%, 80%, and 100%, respectively. Examinations were separated by an interval of 50 to 60 minutes. The time concentration curves for both tissue and arteries were derived according to Equation 2. We predicted that the area under the arterial and tissue time concentration curves would be proportional to the amount of contrast material injected if Equation 2 were valid in both cases.

III. Comparing rCBV Values.—Assuming Equation 2 is valid for both tissues and arteries, we substitute Equation 2 into Equation 1 to obtain an expression for fractional

rCBV (V_f):

$$3) \qquad V_f = \frac{k_{tiss}}{k_{art}} \cdot \frac{\int_0^\infty \ln \frac{S_{tiss}(t)}{S_{tiss}(0)}}{\int_0^\infty \ln \frac{S_{art}(t)}{S_{art}(0)}},$$

where S_{tiss} and S_{art} represent the respective tissue and artery signal intensities at a given time, and k_{tiss} and k_{art} represent the respective calibration constants. If the prestimulation and poststimulation rCBV values are compared in a ratio rather than a difference, then it is not necessary to know the proportionality factors, k_{tiss} or k_{art} in Equation 3, as these calibration terms are constants and will cancel out in the ratio V_{fpre}/V_{fpost}. This ratio comparison would be valid for interpatient comparisons also, assuming the ratio k_{tiss}/k_{art} were the same for all patients. On the other hand, if our aim were to estimate the absolute fractional rCBV itself rather than compare two values in a ratio, we would have to assume a value for k_{tiss}/k_{art} or obtain one empirically. In a previous study, this value was assumed to be 1 for all patients, yielding reasonable mean estimates of absolute rCBV in gray and white matter (15). This same assumption is made in our study for calculation of absolute fractional rCBV. Note that rCBV is described in percentages or fractional rCBV rather than in units of milliliters per 100 g of brain tissue. This practice has become more common in recent reports of positron emission tomography and MR imaging studies (16, 17).

Subjects

Our study was approved by the Intramural Research Review Board of the National Institutes of Neurological Disorders and Stroke, National Institutes of Health, Bethesda, Md. Forty-one healthy subjects ranging in age from 23 to 82 years (mean age, 44 years ± 20) were recruited from the community. All subjects had normal findings on a screening examination, which consisted of a full medical and neurologic history and physical. The exclusion criteria included a history or evidence of cardiovascular disease, diabetes, hypertension, head trauma, previous central nervous system (CNS) infections, exposure to CNS toxins, metabolic or endocrine diseases, and psychiatric distress. Written informed consent was obtained from all subjects.

Study Design

In 30 volunteers, the effect of acetazolamide was investigated; in 10 volunteers, a saline placebo was used in place of acetazolamide to control for the influence of residual contrast (18) or placebo effect. Imaging was performed before and 50 to 60 minutes after intravenous administration of acetazolamide (15 mg/kg in 10 mL) or saline placebo (10 mL). The subjects did not know whether they received acetazolamide or placebo. The perfusion images were analyzed to calculate fractional rCBV for gray and white matter before and after acetazolamide administration. The remaining volunteer was examined with a single-section technique with better spatial resolution to evaluate its effects on estimation of rCBV.

Imaging Protocol

A 20-gauge intravenous catheter was placed in an antecubital vein and connected to an MR-compatible double syringe prototype power injector (Medrad, Pittsburgh, Pa) containing gadopentetate dimeglumine in one syringe and normal saline in the other. The maximal flow rate of 6 mL/s was used. Imaging was performed on a 1.5-T MR system using a standard quadrature head coil. Before injection, routine images were obtained using short repetition time spin-echo and double-echo long repetition time fast spin-echo techniques. Dynamic MR imaging was performed using a 3-D FS-burst sequence (65/42.5 [repetition time/echo time], flip angle of 90°) in a 45° coronal oblique plane. This oblique acquisition plane was necessary to optimize gradient strength to maximize the field of view in the section-select direction (1). The midsagittal section on the short-repetition-time images was used to locate the center of the volume of acquisition at the posterior commissure. The transmit-and-receive gains were set manually to maintain the same parameters from scan to scan. A total of 40 brain volumes (voxel size, 4.0 × 4.0 × 6.1 mm; matrix, 40 × 48 × 36) were obtained during the bolus injection, approximately 2.1 seconds per volume, for a total imaging time of about 1½ minutes. The bolus injection was started 20 seconds into the acquisition using a dose of 0.1 mmol/kg gadopentetate dimeglumine at 6.0 mL/s, followed by a 24-mL normal saline flush at 6.0 mL/s. After this baseline imaging session, the subject was administered acetazolamide (15 mg/kg intravenously). Following a 50 to 60 minute (mean, 50 minutes ± 9) rest period outside the magnet, the subject was imaged again with a short repetition time sagittal localizer followed by a second bolus of contrast material with FS-burst dynamic imaging.

For the subject studied with the single-section higher resolution technique, the imaging protocol was the same as that for the other 40 volunteers studied with FS-burst, except for the dynamic imaging sequence, which consisted of a spoiled gradient-echo (SPGR) technique (30/25, 15° flip angle, 24-cm field of view, 128 × 128 matrix). Parameters were set to match the temporal resolution, section thickness, and scanning plane of the FS-burst sequence. Only a single examination was performed, and no acetazolamide was administered to this subject.

Image Analysis

Reconstruction and analysis of the contrast-enhanced dynamic MR images were performed on a UNIX-based workstation (Hewlett Packard, Corvallis, Ore) using Interactive Data Language (Research Systems, Boulder, Colo) software. For each of the 40 FS-burst volunteers, both

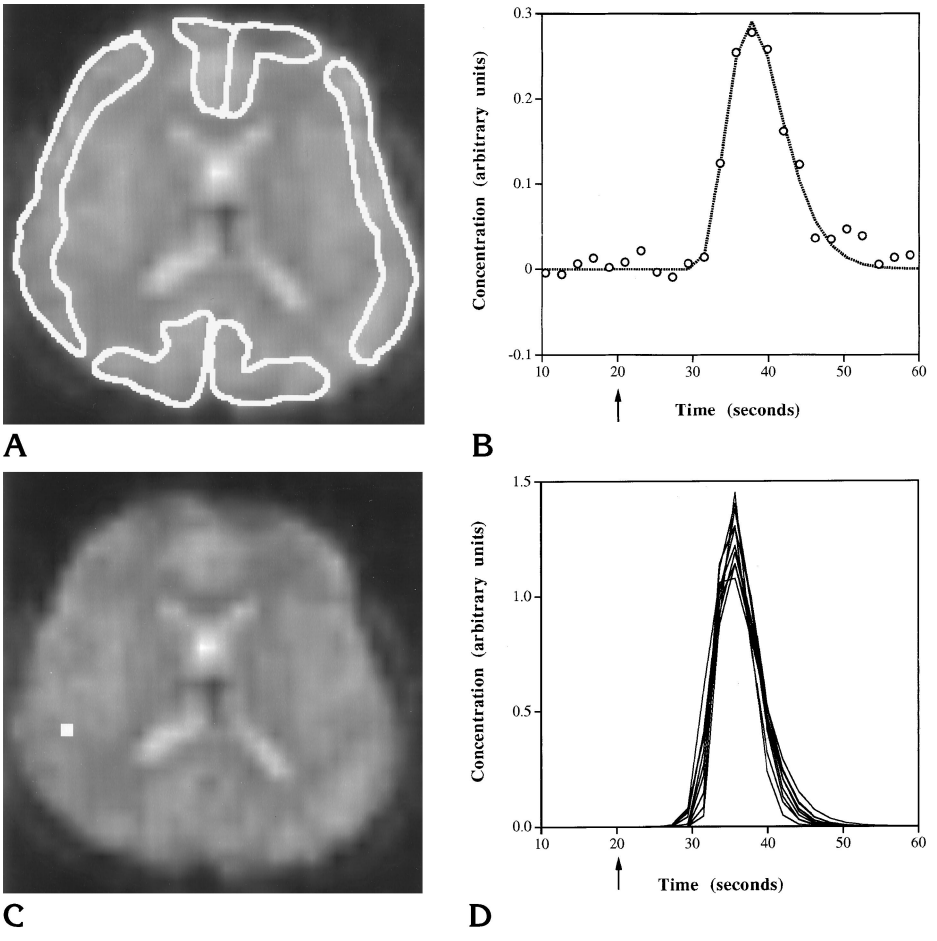

Fig 1. *A*, Dynamic MR image with regions of interest in the medial frontal, frontoparietal, and occipital gray matter, corresponding to the anterior, middle, and posterior cerebral artery vascular territories, respectively.

B, Concentration time plot shows the original data points and fitted curve for a representative gray matter region of interest. *Arrow* indicates time of injection.

C, Dynamic MR image with representative voxel (*white square*) in the region of major branches of the right middle cerebral artery, chosen by algorithm to obtain parameters for arterial input curve.

D, Fitted concentration time plots of 10 voxels selected for arterial input curves.

baseline and postacetazolamide data sets were registered to the first volume of the baseline data set using an intensity-based trilinear interpolation algorithm (19). The images were then resectioned from the 45° coronal oblique plane to the axial plane, again using a linear interpolation technique (20).

Using the first volume (to which all the other volumes were now registered) as a reference, regions of interest (ROIs) were drawn in each hemisphere corresponding to the major cortical cerebral vascular distributions and the supraventricular white matter (21). The gray matter regions were as follows: medial frontal (corresponding to the anterior cerebral artery territory), frontoparietal (middle cerebral artery territory), and occipital (posterior cerebral artery territory) (Fig 1A). Time signal intensity curves were generated for each voxel in the ROI and averaged into a single time signal intensity curve over the 40 time points. This curve was then converted to a time concentration curve using Equation 2. The baseline signal intensity was obtained from averaging the signal intensity of time points 3 through 9. The concentration time curve was then fit in a semiautomated fashion with a γ variate function using a nonlinear least-squares regression method (22, 23). Areas under the fitted tissue time concentration curves were obtained for each ROI (Fig 1B).

To standardize the process of obtaining an arterial input function despite poor spatial resolution, an algorithm was empirically developed to select out arterial voxels on the basis of highest, earliest, and narrowest curve peak. It was recognized that, in addition to selecting arterial voxels, such a criterion might also select voxels in the parenchyma immediately adjacent to large vessels, since these areas may experience a large drop in signal intensity from the local susceptibility effects of the adjacent vessel. The algorithm was as follows: time signal intensity curves for each voxel in the brain were evaluated and 175 curves with the greatest decrease in signal intensity were initially chosen. From these curves, 20 were selected on the basis of the earliest times to peak signal reduction. These 20 curves were converted to time concentration curves and fitted with γ variate functions as described above. From the 20 fitted curves, 10 curves with the shortest mean transit times were selected. The areas under these 10 curves were averaged together to obtain a single area for an arterial input function. This area parameter was used in normalizing the tissue area values from all ROIs in the brain (Fig 1C and D).

Areas for the tissue ROI and arterial input function were tabulated on a spread sheet (Excel, Microsoft Corp, Redmond, Wash), in which absolute fractional rCBV values were calculated according to Equation 1, for gray and

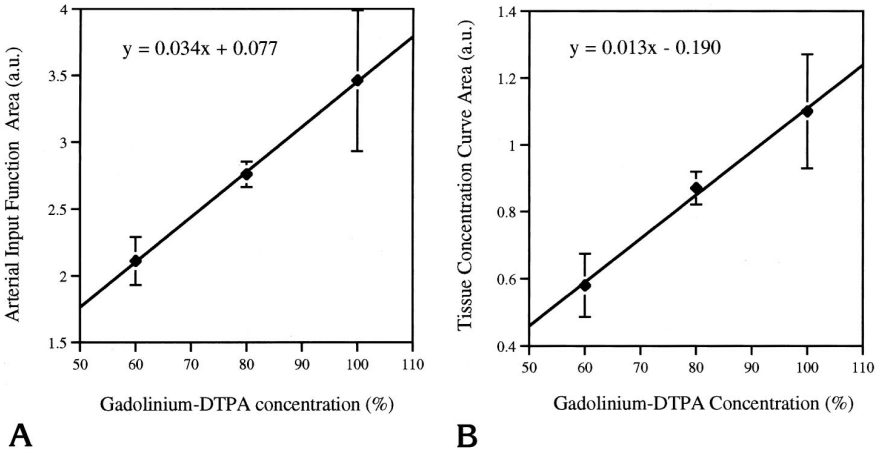

Fig 2. Scatterplots show the linear relationship between the area under the concentration time curve and the percentage gadolinium-DTPA concentration of the injected contrast agent/normal saline mixture. *A* is the arterial input curve; *B* is the tissue curve (gray matter). Error bars show standard deviation.

white matter in general, as well as for each gray matter region. The values for general gray matter were obtained by averaging the individual gray matter regions. All fractional rCBV values were multiplied by a factor of 0.73 to adjust for the difference in percentage of plasma volume between tissues and arteries accountable by different hematocrits (24).

For the single-section SPGR study, only a baseline data set was obtained. ROIs were drawn along the gray matter cortical ribbon and in the white matter. Areas under the fitted tissue time concentration and arterial input function curves were obtained as described above.

Data Analysis

All data were expressed as means and standard deviations. The preacetazolamide and postacetzolamide rCBV values were compared using Student's *t* test (paired) within the treatment and control group. Comparison of the response between the acetazolamide and saline control group was performed with a repeated measures analysis of variance. Statistical significance was defined as $P < .05$.

Fractional cerebral blood volume measurements in 40 healthy volunteers before and after drug challenge (acetazolamide versus saline control)

	Before Challenge, %	After Challenge, %	Mean Change, %
Acetazolamide (n = 30)			
Gray matter	22.2 ± 3	27.3 ± 6	23.0 ($P < .05$)
Medial frontal	22.8 ± 5	29.3 ± 7	28.5 ($P < .05$)
Frontoparietal	21.9 ± 4	27.0 ± 6	23.3 ($P < .05$)
Occipital	21.8 ± 4	25.7 ± 6	17.9 ($P < .05$)
White matter	12.0 ± 3	15.9 ± 4	32.5 ($P < .05$)
Saline control (n = 10)			
Gray matter	21.9 ± 3	22.6 ± 2	3.2 (NS)
Medial frontal	22.4 ± 4	23.8 ± 3	6.3 (NS)
Frontoparietal	21.6 ± 4	22.3 ± 2	3.2 (NS)
Occipital	21.7 ± 2	21.7 ± 3	0.0 (NS)
White matter	12.0 ± 2	13.5 ± 2	12.5 (NS)

Note.—NS indicates not significant.

Results

Relationship between MR Signal and Contrast Agent Concentration

The relationship between concentration of contrast agent and area under the arterial and tissue time concentration curves is shown in Figure 2. This figure demonstrates a linear relationship between the concentration of injected contrast agent and the area under the arterial and tissue concentration curves as determined by Equation 2. We therefore felt confident that using Equation 2 to convert signal intensities to contrast agent concentrations for arteries as well as tissue would not introduce a significant nonlinear bias in estimations of cerebral blood volume.

Baseline rCBV

The mean baseline value for fractional rCBV for all 40 patients in the 3-D FS-burst study was 22% ± 3% for gray matter and 12% ± 2% for white matter. There was a statistically significant difference between these values. The mean gray to white matter rCBV ratio was 1.84. The baseline rCBV values within gray matter, however, did not differ significantly by region.

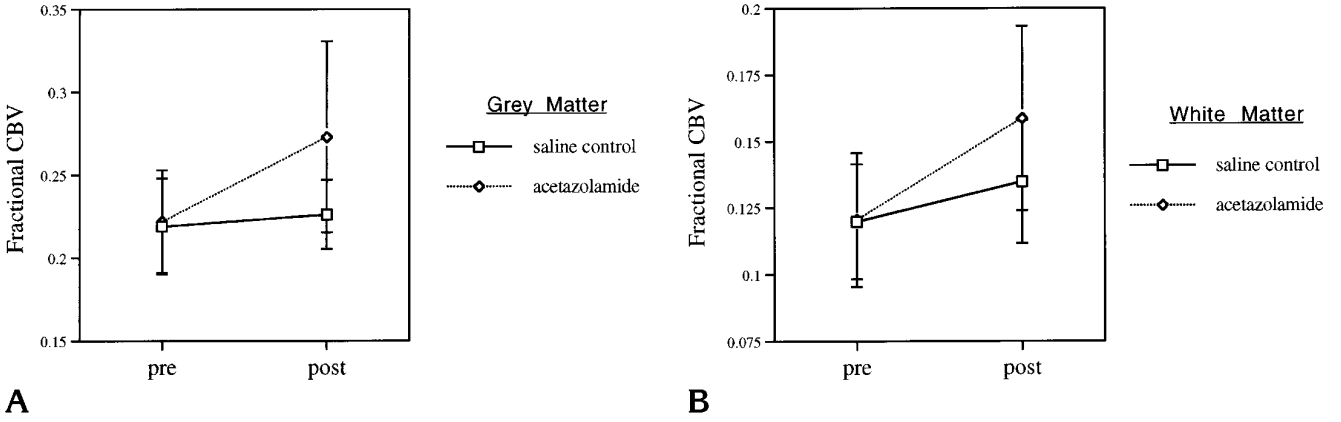

Fig 3. Change in fractional cerebral blood volume (rCBV) in response to acetazolamide versus saline control for gray matter (*A*) and white matter (*B*). Error bars show standard deviation.

Drug Effect

The baseline and postinjection fractional rCBV values for the acetazolamide and saline control groups are shown in the Table. There was a statistically significant increase in rCBV for all regions for the acetazolamide group. Furthermore, this increase was significantly different from that of the saline control group, in which there was no statistically significant change (Fig 3). Reactivity to acetazolamide was highest in the medial frontal gray matter region and differed significantly from that in the frontoparietal and occipital gray matter regions ($P < .05$).

Single-Section Higher Resolution Study

The average baseline values for fractional rCBV for the single-section SPGR study was 13% for gray matter and 5% for white matter. The gray-to-white-matter rCBV ratio was 2.62.

Discussion

Our data in healthy volunteers show that it is possible to detect whole-brain acetazolamide-induced changes in rCBV on a conventional gradient 1.5-T MR system, aided by an independent workstation and customized software, using dynamic contrast imaging with FS-burst. We found a statistically significant increase in rCBV of 23% for gray matter and 33% for white matter in the acetazolamide group, and no significant increases in the saline control group. These results are consistent with those from previous studies using contrast-enhanced perfusion MR imaging and other methods to measure rCBV, such as xenon CT and single-photon emission CT (SPECT) (18, 25, 26)(G. D. Graham, J. Zhong, R. T. Constable, J. W. Prichard, J. C. Gore, "Comparison of Gadolinium Contrast Bolus and BOLD Assessments of Acetazolamide Induced Changes in Human Cerebral Perfusion," presented at the annual meeting of the Society of Magnetic Resonance, San Francisco, Calif, August 1994). Such studies in healthy volunteers reveal a wide range of response (from 10% to 65%) to acetazolamide stimulation for gray and white matter combined. Studies looking at gray and white matter separately have found a greater percentage of increase in rCBV in white matter versus gray matter, similar to our findings (27)(E. Rostrup, H. B. W. Larsson, P. B. Toft, P. Ring, K. Garde, O. Henriksen, "A Contrast Agent Study of Changes in CBV Induced by Hypercapnia," presented at the annual meeting of the Society of Magnetic Resonance, San Francisco, Calif, August 1994). These studies used carbon dioxide as a vasodilator, which is thought to work with a mechanism similar to that of acetazolamide (9).

In addition to gray and white matter differences in baseline rCBV and reactivity to acetazolamide, we also examined regional gray matter differences. We were unable to show significant regional gray matter differences in baseline rCBV, consistent with previous SPECT studies (27). There were, however, significant regional differences in reactivity to acetazolamide. The percentage of change in rCBV was highest in the medial frontal gray matter region, followed by the frontoparietal and occipital re-

gions. These findings also agree with those of previous studies of rCBV changes induced by acetazolamide or hypercapnia, using dynamic contrast MR imaging, in which changes in rCBV were also greater in frontal gray matter (Graham et al, "Comparison. . ."; Rostrup et al, "A Contrast Agent Study. . .").

Such regional gray matter changes in rCBV, however, are reciprocal to the pattern of changes in regional cerebral blood flow (rCBF) measured by SPECT, where greater response to acetazolamide is found in the occipital region, followed by the parietal then frontal regions (28). Studies looking at the effects of CO_2 changes in rhesus monkeys have shown that rCBV and rCBF are closely related. The relationship between rCBF and rCBV, however, is not linear (29) and may reflect the multiple mechanisms of action attributed to acetazolamide and hypercapnia. Increased blood flow in these cases is believed to result from decreased smooth muscle tone in artery and arteriole walls, reducing resistance in the arterial circulation and increasing flow through the capillary bed (30). Increased blood into the capillary bed expands capillary diameter but also results in recruitment of additional capillaries (31). Although capillary recruitment results in an increase in rCBV, it also causes a relative increase in the average length of the path the blood must traverse. This translates into greater overall resistance in the capillary bed, according to Poiseuille's law (32), which somewhat offsets the augmentation in flow from increases in capillary diameter and number. Regions with greater capillary recruitment (and, hence, greater increases in rCBV) will diminish the amount of acetazolamide-induced increase in rCBF. A differential regional response to acetazolamide is consistent with the heterogeneous structure of the cortex (33) and suggests the possibility of significant regional variability in capillary capacitance, which may reflect the differing physiological demands of various brain regions.

Although our calculated acetazolamide-induced percentages of increase in rCBV are comparable to values obtained with the use of other techniques reported in the literature, our rCBV estimates themselves are higher (roughly 20% combined gray and white fractional rCBV in this study compared with about 5% reported in the literature) (26, 29, 34). The main reason for this appears to be partial volume effects from poor spatial resolution of 3-D FS-burst, leading to systematic underestimation of the area under the arterial input function. In the selected arterial voxels there is most likely volume averaging of the artery with adjacent brain parenchyma. The large voxels ($4.0 \times 4.0 \times 6.11$ mm) cannot be completely contained within even the largest of cerebral arteries in the imaging volume. Consequently, the area under the arterial input function is underestimated, leading to an overestimation of the fractional rCBV (see Equation 1). The comparison analysis with a single-section gradient-echo technique shows how volume averaging from a large voxel size might cause overestimation of fractional rCBV. The fractional rCBV values were consistently smaller (13% for gray matter and 5% for white matter) compared with the average values obtained with the 3-D FS-burst technique (22% and 12% for gray and white, respectively). The rCBV values for the single-section gradient-echo technique, although still overestimated, compare favorably with values obtained with a similar technique using dual gradient-echo sections (15). Thus, comparison with higher resolution studies suggests that volume averaging of the arterial input function voxels with adjacent tissue voxels plays a considerable role in the overestimation of rCBV with the FS-burst technique.

Although volume averaging plays a role in overestimations of absolute rCBV, it should not present a problem in ratio comparisons of values between different patients or between different examinations of the same patient, if volume averaging affects all rCBV values the same way. The linear relationship between the injected concentration of contrast agent and our measurement of the arterial input function and tissue area (Fig 2) suggests that all rCBV estimates will be biased by the same multiplicative factor. Thus, quantitative intersubject or intrasubject rCBV ratio comparisons, such pre- to postacetazolamide challenge, are valid. It has been suggested that the linear relationship of Equation 2 may break down at peak contrast concentrations in large vessels (Hedehus et al, "The Relationship..."); however, our data (Fig 2) suggest that using Equation 2 to convert signal intensities to contrast agent concentrations for arteries and for tissue does not introduce a significant nonlinear bias in estimations of rCBV.

A second though probably less influential reason for overestimations of absolute rCBV ap-

plies generally to dynamic susceptibility contrast MR imaging, regardless of the spatial resolution. We, as well as other investigators who have attempted to quantify absolute rCBV with the dynamic susceptibility contrast MR technique, assume that the ratio of the proportionality constants, k_{tiss}/k_{art}, in Equation 3 is equal to 1 (15). This assumption, however, may not be valid. To the extent this is not true, calculated absolute rCBV will be biased.

In summary, we have shown that it is possible to detect changes in rCBV due to acetazolamide on a conventional gradient 1.5-T MR system aided by an independent workstation and customized software using dynamic contrast imaging with FS-burst. Such changes may be used to quantify cerebrovascular reserve across the entire brain. The penalty incurred for whole-brain coverage on a conventional scanner was loss of spatial resolution and systematic overestimation of absolute rCBV values. However, this technique is still well suited for intersubject and intrasubject ratio comparisons, and represents a rapid, readily available way of obtaining whole-brain quantitative hemodynamic information.

Acknowledgments

We thank Alan McLaughlin and Chrit Moonen for helpful discussion of tracer kinetic theory and MR contrast mechanisms, and Jeanette Black, Karen Bove, Renee Hill, and Bobbi Lewis for technical assistance. We also acknowledge Medrad for providing the use of a prototype dual-head MR-compatible mechanical injector.

References

1. Duyn JH, van Gelderen P, Barker P, Frank JA, Mattay VS, Moonen CT. 3D bolus tracking with frequency-shifted BURST MRI. *J Comput Assist Tomogr* 1994;18:680–687
2. Haase A, Frahm J, Matthei D, Haenicke W, Merboldt K. FLASH imaging: rapid NMR imaging using low flip-angle pulses. *J Magn Reson* 1986;67:258–266
3. Moonen CT, Liu G, van Gelderen P, Sobering G. A fast gradient-recalled MRI technique with increased sensitivity to dynamic susceptibility effects. *Magn Reson Med* 1992;26:184–189
4. Moonen CT, Barrios FA, Zigun JR, et al. Functional brain MR imaging based on bolus tracking with a fast $T2^*$-sensitized gradient-echo method. *Magn Reson Imaging* 1994;12:379–385
5. Sorensen AG, Buonanno FS, Gonzalez RG, et al. Hyperacute stroke: evaluation with combined multisection diffusion-weighted and hemodynamically weighted echo-planar MR imaging. *Radiology* 1996;199:391–401
6. Duyn JH, van Gelderen P, Liu G, Moonen CTW. Fast volume scanning with frequency-shifted BURST MRI. *Magn Reson Med* 1994;32:429–432
7. Rosen B, Belliveau J, Chien D. Perfusion imaging by nuclear magnetic resonance. *Magn Reson Q* 1989;5:263–281
8. Rogg J, Rutigliano M, Yonas H, Johnson DW, Pentheny S, Latchaw RE. The acetazolamide challenge: imaging techniques designed to evaluate cerebral blood flow reserve. *AJNR Am J Neuroradiol* 1989;10:803–810
9. Yonas H, Pindzola RR. Physiological determination of cerebrovascular reserves and its use in clinical management. *Cerebrovasc Brain Metab Rev* 1994;6:325–340
10. Ehrenreich DL, Burns RA, Alman RW, Fazekas JF. Influence of acetazolamide on cerebral blood flow. *Arch Neurol* 1961;5:125–130
11. Axel L. Cerebral blood flow determination by rapid-sequence computed tomography. *Radiology* 1980;137:679–686
12. Fisel CR, Ackerman JL, Buxton RB, et al. MR contrast due to microscopically heterogeneous magnetic susceptibility: numerical simulations and applications to cerebral physiology. *Magn Reson Med* 1991;17:336–347
13. Kennan RP, Zhong J, Gore JC. Intravascular susceptibility contrast mechanisms in tissues. *Magn Reson Med* 1994;31:9–21
14. Weisskoff RM, Zuo CS, Boxerman JL, Rosen BR. Microscopic susceptibility variation and transverse relaxation: theory and experiment. *Magn Reson Med* 1994;31:601–610
15. Rempp M, Gunnar B, Wenz F, Becker C, Guckel F, Lorenz W. Quantification of regional cerebral blood flow and volume with dynamic susceptibility contrast-enhanced MR imaging. *Radiology* 1994;193:637–641
16. Leenders KL, Perani D, Lammertsma AA, et al. Cerebral blood flow, blood volume and oxygen utilization: normal values and effect of age. *Brain* 1990;113:27–47
17. Hacklander T, Reichenbach JR, Hofer M, Modder U. Measurement of cerebral blood volume via the relaxing effect of low-dose gadopentetate dimeglumine during bolus transit. *AJNR Am J Neuroradiol* 1996;17:821–830
18. Levin JM, Kaufman MJ, Ross MH, et al. Sequential dynamic susceptibility contrast MR experiments in human brain: residual contrast agent effects, steady state, and hemodynamic perturbation. *Magn Reson Med* 1995;34:655–663
19. Woods RP, Cherry SR, Mazziotta JC. Rapid automated algorithm for aligning and reslicing PET images. *J Comput Assist Tomogr* 1992;16:620–633
20. Gonzalez RC, Woods RE. Image restoration. In: *Digital Image Processing*. Reading, Mass: Addison-Wesley; 1992:300–301
21. Latchaw RE. *MR and CT Imaging of the Head, Neck, and Spine*. St Louis, Mo: Mosby; 1991
22. Thompson HK, Starmer CF, Whalen RE, McIntosh HD. Indicator transit time considered as a gamma variate. *Circ Res* 1964;14:502–515
23. Bevington PR. Data Reduction and Error Analysis for the Physical Sciences. New York, NY: McGraw-Hill; 1969:366
24. Everett N, Simmons B, Laster E. Distribution of blood (Fe^{59}) and plasma (I^{131}) volumes of rats determined by liquid nitrogen freezing. *Circ Res* 1956;4:419–424
25. Steiger HJ, Aaslid R, Stooss R. Dynamic computed tomographic imaging of regional cerebral blood flow and blood volume: a clinical pilot study. *Stroke* 1993;24:591–597
26. Sabatini U, Celsis P, Viallard G, Rascol A, Marc-Vergnes J. Quantitative assessment of cerebral blood volume by single-photon emission computed tomography. *Stroke* 1991;22:324–330
27. Greenberg JH, Alavi A, Reivich M, Kuhl D, Uzzel B. Local cerebral blood volume response to carbon dioxide in man. *Circ Res* 1978;43:324–331

28. Leinsinger G, Piepgras A, Einhaupl K, Schmiedek P, Kirsch C. Normal values of cerebrovascular reserve capacity after stimulation with acetazolamide measured by xenon 133 single-photon emission CT. *AJNR Am J Neuroradiol* 1994;15:1327–1332
29. Grubb RL, Raichle ME, Higgins CS, Eichling JO. Measurement of regional cerebral blood volume by emission tomography. *Ann Neurol* 1978;4:322–328
30. Mchedlishvili G. *Arterial Behavior and Blood Circulation in the Brain*. New York, NY: Plenum Press; 1986:338
31. Villringer A, Them A, Lindauer U, Einhaupl K, Dirnagl U. Capillary perfusion of the rat brain cortex. *Circ Res* 1994;75:55–62
32. Burns DM, MacDonald SGG. *Physics for Biology and Pre-Medical Students*. London, England: Addison-Wesley; 1970
33. Brodmann K. Vergleichende Lokalisationlehre der Groshirnrinde in ihren. In: *Prinzipien dargestelt auf Grund des Zellenbaues*. Leipzig, Germany: Barth; 1909
34. Phelps ME, Huang SC, Hoffman EJ. Validation of tomography measurement of cerebral blood volume with C-11 labeled carboxyhemoglobin. *J Nucl Med* 1979;20:328–334